

Formation of the Abundance Boundaries of the Heavier Neutron-capture Elements in Metal-poor Stars

Guochao Yang¹, Hongjie Li^{1,2}, Nian Liu³, Lu Zhang⁴, Wenyuan Cui¹, Yanchun Liang⁵, Ping Niu^{1,6} and Bo Zhang^{1,*}

ABSTRACT

The abundance scatter of heavier r-process elements ($Z \geq 56$) relative to Fe ($[r/Fe]$) in metal-poor stars preserves excellent information of the star formation history and provides important insights into the various situations of the Galactic chemical enrichment. In this respect, the upper and lower boundaries of $[r/Fe]$ could present useful clues for investigating the extreme situations of the star formation history and the early Galactic chemical evolution. In this paper, we investigate the formation of the upper and lower boundaries of $[r/Fe]$ for the gas clouds. We find that, for a cloud from which metal-poor stars formed, the formation of the upper limits of $[r/Fe]$ is mainly due to the pollution from a single main r-process event. For a cloud from which metal-poor stars formed, the formation of the lower limits of $[r/Fe]$ is mainly due to the pollution from a single SN II event that ejects primary Fe.

Subject headings: nuclear reactions, nucleosynthesis, abundances – stars: abundances – stars: massive

1. Introduction

The neutron-capture (n-capture) process which dominantly creates heavy elements consists of the slow n-capture process (s-process) and the rapid n-capture process (r-process) (Burbidge et al. 1957). The s-process consists of the weak s-process and the main s-process. Massive stars are the astrophysical sites of the weak s-process which mainly produces the lighter n-capture elements (e.g., Sr, Y and Zr) (Lamb et al. 1977; Raiteri et al. 1991, 1993). Asymptotic giant branch stars are the astrophysical sites of the main s-process which produces both the lighter and heav-

ier n-capture elements (Busso et al. 1999). The r-process consists of the weak r-process (or “lighter element primary process” (LEPP), Travaglio et al. 2004) and main r-process (Cowan et al. 1991). Because the yields of both the weak r-process (or LEPP) elements and the light elements have primary nature, the weak r-process is suggested to occur in SNe II with the progenitor mass $M > 10M_{\odot}$ (Travaglio et al. 2004; Montes et al. 2007). The main r-process is considered to associate with the final stages of massive star evolution, yet the actual astrophysical sites have not been confirmed (Snedden et al. 2008; Ishimaru et al. 2015; Goriely & Janka 2016). Two astrophysical sites of the main r-process are paid attention: (1) the SNe II with the progenitor mass $M \approx 8 - 10M_{\odot}$ (Travaglio et al. 1999; Wanajo et al. 2003; Qian & Wasserburg 2007) and (2) neutron star mergers (NSMs) (Lattimer & Schramm 1974; Eichler et al. 1989; Tsujimoto & Shigeyama 2014a,b). The r-process abundances of the solar system have been obtained by Käppeler et al. (1989) and Arlandini et al. (1999) using the residual approach. The two components of n-capture process have been found in the elemental abundances of metal-poor stars (Wasserburg et al. 1996; Qian et al. 1998). Based on the elemental abundances of the main r-process stars

¹Department of Physics, Hebei Normal University, NO. 20 Road East of 2nd Ring South, Shijiazhuang, 050024, China

²School of Sciences, Hebei University of Science and Technology, Shijiazhuang, 050018, China

³Astronomy Department, Beijing Normal University, Beijing, 100875, China

⁴College of Mathematics and Information Science, Hebei Normal University, Shijiazhuang, 050024, China

⁵Key Laboratory of Optical Astronomy, National Astronomical Observatories, Chinese Academy of Sciences, Beijing, 100012, China

⁶Department of Physics, Shijiazhuang University, Shijiazhuang 050035, China

*E-mail address: zhangbo@mail.hebtu.edu.cn

and the weak r-process stars, adopting the iterative method, Li et al. (2013b) and Hansen et al. (2014) derived the abundances of the main r-process and the weak r-process.

Elemental abundances of metal-poor stars reflect the chemical composition of the natal clouds polluted by different nucleosynthetic processes. Truran (1981) studied the abundances of the r-process elements in the Galactic halo stars and suggested that the r-process enrichment in metal-poor stars originates from the early massive stars. Because of the secondary nature (i.e., the yields are correlated with the initial stellar metallicity), the s-process contributions to the n-capture elements in interstellar medium (ISM) are negligible at low metallicities ($[\text{Fe}/\text{H}] \leq -1.5$). In this case, the n-capture elements of metal-poor stars dominantly come from the r-process (Travaglio et al. 1999; Burris et al. 2000). Study of the abundance characteristics of the n-capture elements in metal-poor stars is significant for understanding the r-process nucleosynthesis and the chemical enrichment history of the early Galaxy. Gilroy et al. (1988) reported that there exists a large $[\text{r}/\text{Fe}]$ scatter for the heavier n-capture elements at low metallicity. They proposed that the scatter reflects the inhomogeneous mixing of products from different nucleosynthetic processes. The large $[\text{r}/\text{Fe}]$ scatter is also shown in more observational work (e.g., McWilliam et al. 1995; Ryan et al. 1996; McWilliam 1998; Sneden et al. 1998; Burris et al. 2000; Honda et al. 2004; Barklem et al. 2005; François et al. 2007; Roederer et al. 2010). Mathews et al. (1992) and Travaglio et al. (1999) calculated the Galactic evolution of the n-capture elements and suggested that the abundances of the heavier r-process elements should be produced by the lower-mass SNe II. Sneden et al. (1994) studied the abundances of the main r-process star CS 22892-052 and ascribed the Eu enrichment in this star to the unmixed chemical composition of the cloud swept up by the SN event. McWilliam et al. (1995) and McWilliam (1998) analyzed the chemical abundances of extremely metal-poor stars. They proposed that the observed abundance dispersions of the heavier n-capture elements indicate the chemical inhomogeneities of the ISM. However, Ryan et al. (1996) suggested that the different gas clouds would be entirely inhomogeneous and the r-process element enrichment in a gas cloud is only due to the pollution from a main r-process event. Tsujimoto et al. (1999) studied the $[\text{Eu}/\text{Fe}]$ scatter in the Galactic halo and suggested that the $[\text{Eu}/\text{Fe}]$ scatter in metal-poor stars

is the integrated results of remnants of the SNe with different progenitor mass. Argast et al. (2000) analyzed the $[\text{Eu}/\text{Fe}]$ pattern of metal-poor stars using the three-dimensional stochastic evolution model. They proposed that (1) the large $[\text{Eu}/\text{Fe}]$ scatter for $[\text{Fe}/\text{H}] < -3.0$ should result from the inhomogeneities of the clouds swept up by the SNe II with different initial mass and (2) the $[\text{Eu}/\text{Fe}]$ scatter decreases with increasing metallicity because of the chemical mixing of the ISM. Travaglio et al. (2001) calculated the Galactic halo evolution considering the chemical mixing of the clouds and the products of SNe. They found that the $[\text{r}/\text{Fe}]$ scatter at low metallicity is the results of inhomogeneous mixing of the ISM and the chemical enrichment of the gas clouds is dominated by the star formation episodes. Fields et al. (2002) presented a simple model to explain the $[\text{Eu}/\text{Fe}]$ scatter for metal-poor stars and suggested that the decreasing $[\text{Eu}/\text{Fe}]$ scatter with increasing metallicity is due to the mixing of the sources produced by different nucleosynthetic events. Cescutti (2008) used the stochastic evolution model to investigate the formation of the $[\text{r}/\text{Fe}]$ scatter in metal-poor stars and suggested that the different $[\text{r}/\text{Fe}]$ dispersions are caused by the massive stars with different mass ($12 \sim 30 M_{\odot}$).

Over the years, NSM is also argued as a plausible astrophysical site of main r-process which leads to the r-process enrichment in metal-poor stars. Based on the observed abundances of lighter r-process elements (i.e., Y and Zr) and heavier r-process element Eu of metal-poor stars, Tsujimoto & Shigeyama (2014a) suggested that (1) the core-collapse supernovae produce the lighter r-process elements and (2) there exist two types of NSMs: one type only produces the heavier r-process elements and the other produces both the lighter and heavier r-process elements. Considering the accretion of ISM and the chemical enrichment of intergalactic medium, Komiya et al. (2014) calculated the chemical evolution of the heavier r-process elements Ba and Eu. They found that both the SNe II and NSMs can reproduce the abundance patterns of the heavier r-process elements of extremely metal-poor stars. Tsujimoto & Shigeyama (2014b) studied the Eu enrichment in the Galactic halo and proposed that the $[\text{Eu}/\text{Fe}]$ scatter in the Galactic halo stars can be explained by the hierarchical galaxy formation model. Furthermore, they suggested that NSMs should be the dominant astrophysical site of the main r-process. Through simulating the chemical and dynamic evolution of NSMs, Rosswog et al. (2014) sug-

gested that the dynamic ejecta of NSMs could produce the heavier r-process elements with $A > 130$. In order to distinguish the products of the SN II and NSM events, Hotokezaka et al. (2015) calculated the abundances of the short-lived element ^{244}Pu and compared the theoretical values with the observed abundances. They proposed that the NSM events can naturally explain the ^{244}Pu abundances and are an excellent candidate of the astrophysical origins of the heavier r-process elements. By comparing the calculated abundances with the observed abundances of CS 22892-052, Ramirez-Ruiz et al. (2015) concluded that NSMs are a favorable source of the heavier r-process elements in CEMP-r stars. They also found that the NSM events could naturally explain the scatter of observed Eu abundances in CEMP-r stars. Based on the discovery of strong r-process enhanced stars in the ultra-faint dwarf galaxy Reticulum II, Ji et al. (2016) suggested that the r-process material in Reticulum II should be produced by the single NSM event. For examining the NSMs as astrophysical origins of the r-process elements in dwarf galaxies, Beniamini et al. (2016a) calculated the proper motion and the time until merger of neutron star binaries. They concluded that (1) more than 50% of neutron star binaries have small proper motion to avoid the pollution of SN ejecta and (2) more than 90% of neutron star binaries merge within 300 Myr. These results indicate that NSMs could be naturally responsible for the observed r-process abundances of the metal-poor stars of the early Galaxy. Based on the hierarchical chemical evolution model, Komiya & Shigeyama (2016) simulated the abundances of the r-process elements for metal-poor stars after considering the pollution of NSM ejecta. They suggested that the NSM scenario can successfully reproduce the $[\text{r}/\text{Fe}]$ scatter for metal-poor stars. Through calculating the rate and yields for the r-process event in dwarf galaxies, Beniamini et al. (2016b) found that the dwarf galaxies and the Milky Way share the same r-process mechanism.

For metal-poor stars, the α elements (e.g., Mg, Si, Ca and Ti) and Fe originate from massive stars (Woosley & Weaver 1995; Kobayashi et al. 2006; Heger & Woosley 2010; Mishenina et al. 2013). To explore the abundance correlations between α elements and main r-process elements, Li et al. (2014) plotted the observed $[\alpha/\text{Eu}]$ as a function of $[\text{Eu}/\text{Fe}]$ for metal-poor stars and found that the observed $[\alpha/\text{Eu}]$ ratios decrease linearly with increasing $[\text{Eu}/\text{Fe}]$ and the slope is close to -1 . The results mean that the abun-

dances of α elements and Fe have no correlation with those of Eu, which indicates that the astrophysical site producing main r-process elements does not produce α elements and Fe. The observational and theoretical results of the previous work imply that the $[\text{r}/\text{Fe}]$ scatter is dominated by more than one factor. Obviously, the upper and lower boundaries of $[\text{r}/\text{Fe}]$ could provide useful clues about the extreme situations of the chemical enrichment of the gas clouds. So the quantitative study of the $[\text{r}/\text{Fe}]$ boundaries in metal-poor stars is important. In this paper, we investigate the formation of the $[\text{r}/\text{Fe}]$ boundaries for the heavier n-capture elements ($Z \geq 56$) of metal-poor stars in § 2. Conclusions are presented in § 3.

2. Abundance Boundaries of $[\text{r}/\text{Fe}]$ for the Heavier n-capture Elements in Metal-poor Stars

Generally, Eu is deemed as a typical main r-process element in the solar system. The left panel of Figure 1 shows the observed $[\text{Eu}/\text{Fe}]$ as a function of $[\text{Fe}/\text{H}]$ for the metal-poor stars (Westin et al. 2000; Cowan et al. 2002; Hill et al. 2002; Johnson 2002; Sneden et al. 2003; Christlieb et al. 2004; Honda et al. 2004; Barklem et al. 2005; Ivans et al. 2006; Honda et al. 2006, 2007; Francis et al. 2007; Lai et al. 2008; Hayek et al. 2009; Aoki et al. 2010; Mashonkina et al. 2010; Roederer et al. 2010, 2014; Hollek et al. 2011; Hansen et al. 2012, 2015; Siqueira-Mello et al. 2012; Cohen et al. 2013; Yong et al. 2013; Mashonkina et al. 2014; Jacobson et al. 2015; Li et al. 2015a,b; Siqueira-Mello et al. 2016). In order to avoid the effect of s-process, we select the sample stars with $[\text{Fe}/\text{H}] \leq -1.5$ and $[\text{Ba}/\text{Eu}] < 0$. The dotted line with -1 slope in the panel represents the sensitivity limit for the observing Eu, which is 0.8 dex lower than that adopted by Travaglio et al. (2001). From the panel we can see that the $[\text{Eu}/\text{Fe}]$ scatter is larger than 2 dex at $[\text{Fe}/\text{H}] = -3.0$, whereas the scatter decreases with increasing metallicity. The observed upper boundary of $[\text{Eu}/\text{Fe}]$ is explicit: it is close to a straight line with the slope ~ -1 for $[\text{Fe}/\text{H}] \lesssim -2.5$, while the decreasing trend flattens for $[\text{Fe}/\text{H}] > -2.5$. On the other hand, the observed lower boundary shows a sharp increasing trend for $[\text{Fe}/\text{H}] \lesssim -2.5$, while the increasing trend flattens for $[\text{Fe}/\text{H}] > -2.5$.

In order to explain the upper and lower boundaries of $[\text{Eu}/\text{Fe}]$ for the metal-poor stars, we consider the initial chemical composition of the gas clouds and the pollution from the two nucleosynthetic events: (1) the main r-process event and (2) the SN II event that ejects

primary Fe (hereafter simply the SN II-Fe event). The main r-process event (e.g., the SN II with the progenitor mass $M \approx 8 - 10M_{\odot}$ or NSM) produces and ejects the main r-process elements (Travaglio et al. 1999; Qian & Wasserburg 2007; Tsujimoto & Shigeyama 2014b). Whereas the SN II-Fe event (i.e., the SN II with the progenitor mass $M > 10M_{\odot}$) mainly produces the weak r-process (or LEPP) elements and ejects light elements and Fe group elements simultaneously (Travaglio et al. 2004; Montes et al. 2007; Li et al. 2013a).

For the main r-process events, although two possible sites (i.e., the SNe II with the progenitor mass $M \approx 8 - 10M_{\odot}$ or NSMs) attract common attention, the actual main r-process sites and corresponding main r-process yields have not been determined. For a gas cloud swept up by a single main r-process event, the relationship between the Eu abundance N_{Eu} and the Fe abundance N_{Fe} is

$$\frac{N_{Eu}}{N_{Fe}} = \left(\frac{A_{Fe}}{A_{Eu}}\right) \left(\frac{M_{SW,rm}X_{Eu} + Y_{Eu}}{M_{SW,rm}X_{Fe}}\right), \quad (1)$$

where $M_{SW,rm}$ is the mass of the cloud. X_{Eu} and X_{Fe} are the initial mass fractions of Eu and Fe in the cloud. Y_{Eu} is the Eu yield of the main r-process event. A_{Eu} and A_{Fe} are the atomic weights of Eu and Fe, respectively. Based on the observed abundances of Ba and Eu, Cescutti et al. (2006) computed the mean [Ba/Fe] and [Eu/Fe] ratios in different [Fe/H] bins. In this work, we adopt the mean [Eu/Fe] ratios presented by Cescutti et al. (2006) as the initial abundance ratios ($[Eu/Fe]_{ini}$) of the gas clouds, which are plotted in the left panel of Figure 1 by the dashed line. The upper limits of [Eu/Fe] of the clouds are calculated for two cases.

Case A: the pollution from the SNe II with the progenitor mass $M \approx 8 - 10M_{\odot}$. The core-collapse SNe should consist of two routes (e.g., Qian & Wasserburg 2007): (1) the Fe core-collapse SNe with the progenitor mass $M \gtrsim 11M_{\odot}$ from which the light elements and Fe group elements are ejected and (2) the O-Ne-Mg core-collapse SNe with the progenitor mass $M \approx 8 - 10M_{\odot}$ in which the light elements and Fe group elements are not produced. The main r-process may take place in O-Ne-Mg core-collapse SNe. In this case, the astrophysical sites ejecting main r-process elements do not eject light elements and Fe group elements. Owing to the high Eu abundance ($[Eu/Fe] = 1.92$) and low metallicity ($[Fe/H] = -3.36$), the sample star SDSS J2357-0052 (Aoki et al. 2010) is taken as the repre-

sentative star and $[Eu/Fe] = 1.92$ is taken as the upper limit at $[Fe/H] = -3.36$. Adopting the Eu yield of the main r-process event $Y_{Eu} = 6.4 \times 10^{-7}M_{\odot}$ (Travaglio et al. 2001), from equation (1) we can derive $M_{SW,rm} = 4.5 \times 10^4M_{\odot}$. Using the derived cloud mass, from equation (1) we can derive the upper limits ($[Eu/Fe]_{up}$) for the clouds with different metallicities which were swept up by the SNe II with the progenitor mass $M \approx 8 - 10M_{\odot}$. The calculated results are shown in the left panel of Figure 1 by the solid line. We can see that the calculated upper boundary is close to a straight line with the slope ~ -1 for $[Fe/H] \lesssim -2.5$, while the decreasing trend flattens for $[Fe/H] > -2.5$. Obviously, the calculated results are consistent with the observed upper boundary of [Eu/Fe] of the sample stars.

Case B: the pollution from NSMs. Based on the NSM scenario, Komiya & Shigeyama (2016) explored the [r/Fe] scatter of metal-poor stars using the hierarchical galaxy formation model. They suggested that the Eu yield of a NSM event is about $1.5 \times 10^{-4}M_{\odot}$ and the mass of the cloud swept up by the single main r-process event is about 10^7M_{\odot} . For the NSM scenario, the Eu yield is about 3 orders of magnitude higher than what is adopted for Case A and the gas mass that Eu is diluted into is also about 3 orders of magnitude higher than what is adopted for Case A. Adopting the Eu yield $Y_{Eu} = 1.5 \times 10^{-4}M_{\odot}$ and the polluted cloud mass $M_{SW,rm} = 10^7M_{\odot}$, we calculate the upper limits of [Eu/Fe] for the clouds swept up by NSMs. The calculated results are plotted in the left panel of Figure 1 by the dotted-dashed line. We can see that the upper boundaries of [Eu/Fe] for the two cases are very similar.

For illustrating the formation of the upper boundary of [Eu/Fe] clearly, in the right panel we use the up arrows to show the jumps of [Eu/Fe]. For the cloud with the initial ratios $[Eu/Fe]_{ini} = -0.59$ and $[Fe/H] = -3.5$, the final ratio $[Eu/Fe]_{up} \approx 2.06$ means that the [Eu/Fe] ratio jumps from -0.59 to 2.06 because of the pollution from the single main r-process event. In this case, the increasing value of [Eu/Fe] reaches about 2.65 dex, since (1) the initial Fe mass fraction X_{Fe} of the cloud is small and (2) the initial Eu mass in the cloud is much lower than the Eu yield of the main r-process event (i.e., $M_{SW,rm}X_{Eu} \ll Y_{Eu}$). On the other hand, for the cloud with the initial ratios $[Eu/Fe]_{ini} = 0.44$ and $[Fe/H] = -1.5$, the final ratio $[Eu/Fe]_{up} \approx 0.60$ means that the increasing value of [Eu/Fe] is only about 0.16 dex. The two reasons

lead to the flat of the upper boundary of [Eu/Fe]: (1) the cloud contains more Fe and (2) the initial Eu mass in the cloud is higher than the Eu yield of the main r-process event (i.e., $M_{SW,rm}X_{Eu} > Y_{Eu}$). The derived results mean that, for a cloud from which metal-poor stars formed, the formation of the upper limit of [Eu/Fe] is mainly due to the pollution from a single main r-process event.

For a gas cloud swept up by a single SN II-Fe event, the relationship between the Eu abundance N_{Eu} and the Fe abundance N_{Fe} is

$$\frac{N_{Eu}}{N_{Fe}} = \left(\frac{A_{Fe}}{A_{Eu}}\right) \left(\frac{M_{SW,pri}X_{Eu}}{M_{SW,pri}X_{Fe} + Y_{Fe}}\right), \quad (2)$$

where $M_{SW,pri}$ is the mass of the cloud. Y_{Fe} is the Fe yield of the SN II-Fe event. We take the typical weak r-process star HD 122563 ([Fe/H] = -2.77 , [Eu/Fe] = -0.52 , Honda et al. 2006) as the representative star and take [Eu/Fe] = -0.52 as the lower limit at [Fe/H] = -2.77 . Adopting the polluted cloud mass $M_{SW,pri} = 6.5 \times 10^4 M_{\odot}$ (Tsujiimoto et al. 1999), from equation (2) we can derive $Y_{Fe} = 0.1 M_{\odot}$. Using the derived Fe yield, from equation (2) we can derive the lower limits ([Eu/Fe]_{lw}) for the clouds with different metallicities, which are shown in the left panel of Figure 1 by the solid line. We can see that the calculated lower boundary shows a sharp increasing trend for [Fe/H] $\lesssim -2.5$ and a mild increasing trend for [Fe/H] > -2.5 . There are some observed [Eu/Fe] ratios that are significantly lower than the calculated lower boundary in the range $-2.5 < [\text{Fe}/\text{H}] < -2.2$. Note that the initial [Eu/Fe] ratio of a cloud takes some effect on the lower limit of [Eu/Fe]. In this work, we take the observed mean [Eu/Fe] ratios as the initial [Eu/Fe] ratios of the clouds. Obviously, the actual initial ratios of the clouds could deviate from the mean ratios. If the actual initial [Eu/Fe] ratio of a cloud swept up by a SN II-Fe event is lower than the mean [Eu/Fe] ratio, the actual lower limit of [Eu/Fe] should be lower than the calculated lower limit plotted in Figure 1. The observed low [Eu/Fe] ratios should imply that the actual initial [Eu/Fe] ratios of these clouds are lower than the mean [Eu/Fe] ratios. Furthermore, because the explosion energy of SNe II depends on their progenitor mass (Kobayashi et al. 2006; Nomoto et al. 2013) and the mass of the clouds swept up by the SNe II increases with increasing explosion energy (Machida et al. 2005), the mass of the clouds swept up by the SNe II with the progenitor mass $M > 10 M_{\odot}$ should be larger than that of the

clouds swept up by the SNe II with the progenitor mass $M \approx 8 - 10 M_{\odot}$.

For illustrating the formation of the lower boundary of [Eu/Fe] clearly, in the right panel we use the inclined arrows to represent the jumps of [Eu/Fe] and [Fe/H]. For the cloud with the initial ratios [Eu/Fe]_{ini} = -0.60 and [Fe/H] = -3.5 , the final ratios [Eu/Fe]_{lw} = -1.25 and [Fe/H] = -2.85 imply that the [Fe/H] ratio jumps from -3.5 to -2.85 because of the pollution from the single SN II-Fe event. In this case, the increasing value of [Fe/H] reaches 0.65 dex, since the initial Fe mass in the cloud is lower than the Fe yield of the SN II-Fe event (i.e., $M_{SW,pri}X_{Fe} < Y_{Fe}$). On the other hand, for the cloud with initial ratios [Eu/Fe]_{ini} = 0.44 and [Fe/H] = -1.5 , the final ratios [Eu/Fe]_{lw} = 0.42 and [Fe/H] = -1.48 mean that the increasing value of [Fe/H] is only 0.02 dex. The two reasons lead to the flat of the lower boundary of [Eu/Fe]: (1) the cloud contains more Eu and (2) the initial Fe mass in the cloud is higher than the Fe yield of the SN II-Fe event (i.e., $M_{SW,pri}X_{Fe} > Y_{Fe}$). The derived results mean that, for a cloud from which metal-poor stars formed, the formation of the lower limit of [Eu/Fe] is mainly due to the pollution from a single SN II-Fe event.

The first generation of very massive stars only produces light elements and Fe group elements (Komiya et al. 2014). This abundance pattern is represented by the prompt (P) component (Qian & Wasserburg 2001) which should be responsible for the origin of light elements and Fe for [Fe/H] $\lesssim -3.5$. For the clouds with [Fe/H] $\gtrsim -3.5$, the element Eu originates from the main r-process events (e.g., the SNe II with the progenitor mass $M \approx 8 - 10 M_{\odot}$ or NSMs) and the element Fe originates from (1) the prompt inventory (P-inventory) of Fe at the early universe (Qian & Wasserburg 2001) and (2) the SN II-Fe events. The effect of the P-inventory became smaller when the SN II-Fe events began to pollute the ISM (Qian & Wasserburg 2001; Li et al. 2013b). On the other hand, for the most stars with [Fe/H] $\lesssim -3.5$, the element Fe should mainly originate from the P-inventory and the observed r-process abundances should be ascribed to the surface pollution by the ISM which had contained r-process material (Komiya et al. 2014; Komiya & Shigeyama 2016).

Figures 2 and 3 show the observed [r/Fe] (r: Ba, La, Ce, Pr, Nd, Sm, Gd, Tb, Dy, Ho, Er, Tm, Yb, Lu, Hf, Os, Ir, Pt, Au and Pb) as a function of [Fe/H] for the metal-poor stars. From the figures we can see that the

observed trends of the upper and lower boundaries of [r/Fe] are similar to those of [Eu/Fe]. For a gas cloud swept up by a single main r-process event, the relationship between the r-process abundance $N_{i,r}$ and the Fe abundance N_{Fe} is:

$$\frac{N_{i,r}}{N_{Fe}} = \left(\frac{A_{Fe}}{A_i}\right) \left(\frac{M_{SW,rm} X_i + Y_{i,rm}}{M_{SW,rm} X_{Fe}}\right), \quad (3)$$

where X_i is the initial mass fraction of the i th element. $Y_{i,rm}$ is the main r-process yield. A_i is the atomic weight. The main r-process yield $Y_{i,rm}$ can be derived as:

$$Y_{i,rm} = \frac{A_i N_{i,rm}^*}{A_{Eu} N_{Eu}^*} Y_{Eu}, \quad (4)$$

where $N_{i,rm}^*$ and N_{Eu}^* are the component abundances, which are adopted from Li et al. (2013b). Using the initial [Eu/Fe] ratios of the clouds adopted from Cescutti et al. (2006) and the component abundances adopted from Li et al. (2013b), we can derive the initial [r/Fe] ratios for the clouds, which are plotted in Figures 2 and 3 by the dashed lines. The upper limits of [r/Fe] of the clouds are also calculated for two cases.

Case A: the pollution from the SNe II with the progenitor mass $M \approx 8 - 10 M_\odot$. Adopting the Eu yield $Y_{Eu} = 6.4 \times 10^{-7} M_\odot$ and the polluted cloud mass $M_{SW,rm} = 4.5 \times 10^4 M_\odot$, from equations (3) and (4) we can derive the upper limits of [r/Fe] for the clouds swept up by the SNe II with the progenitor mass $M \approx 8 - 10 M_\odot$. The results are plotted in Figures 2 and 3 by the solid lines.

Case B: the pollution from NSMs. Adopting the Eu yield $Y_{Eu} = 1.5 \times 10^{-4} M_\odot$ and the polluted cloud mass $M_{SW,rm} = 10^7 M_\odot$, we derive the upper limits of [r/Fe] for the clouds swept up by NSMs, which are plotted in Figures 2 and 3 by the dotted-dashed lines. Obviously, the calculated upper boundaries are close to the observed upper boundaries of [r/Fe] of the sample stars. These results could provide more supports for the suggestion that the formation of the upper limits of [r/Fe] in a cloud is mainly due to the pollution from a single main r-process event.

For a gas cloud swept up by a single SN II-Fe event, the relationship between the r-process abundance $N_{i,r}$ and the Fe abundance N_{Fe} is:

$$\frac{N_{i,r}}{N_{Fe}} = \left(\frac{A_{Fe}}{A_i}\right) \left(\frac{M_{SW,pri} X_i + Y_{i,pri}}{M_{SW,pri} X_{Fe} + Y_{Fe}}\right), \quad (5)$$

where $Y_{i,pri}$ is the primary yield of the i th element from the SN II-Fe event. The primary yield $Y_{i,pri}$ can

be derived as:

$$Y_{i,pri} = \frac{A_i N_{i,pri}^*}{A_{Fe} N_{Fe}^*} Y_{Fe}, \quad (6)$$

where $N_{i,pri}^*$ and N_{Fe}^* are the component abundances, which are adopted from Li et al. (2013b). Adopting the derived Fe yield $Y_{Fe} = 0.1 M_\odot$ and the polluted cloud mass $M_{SW,pri} = 6.5 \times 10^4 M_\odot$, from equations (5) and (6) we can derive the lower limits of [r/Fe] for the clouds with different metallicities. The results are plotted in Figures 2 and 3 by the solid lines. We can see that the lines are close to the observed lower boundaries of [r/Fe] of the sample stars. The results also mean that the formation of the lower limits of [r/Fe] in a cloud is mainly due to the pollution from a single SN II-Fe event.

3. Conclusions

The [r/Fe] scatter of the heavier n-capture elements in metal-poor stars preserves excellent information of the star formation history and provides important insights into the various situations of the Galactic chemical enrichment. In this respect, the upper and lower boundaries of [r/Fe] could present useful clues for investigating the extreme situations of the chemical enrichment of the clouds. In this paper, we investigate the formation of the upper and lower boundaries of [r/Fe] for the clouds. The main results are listed as follows:

1. Based on the assumptions of (1) the progenitor of the main r-process event does not produce Fe and (2) the yields of the main r-process event possess the primary nature (i.e., the yields are uncorrelated with the initial stellar metallicity), we find that the observed upper boundaries of [r/Fe] can be explained. For the clouds with the initial metallicities $[Fe/H] \lesssim -2.5$, the upper boundaries of [r/Fe] are close to straight lines with slopes ~ -1 , since the mass of the initial r-process elements in each of the clouds is lower than the yields of the single main r-process event. On the other hand, for the clouds with the initial metallicities $[Fe/H] > -2.5$, the upper boundaries of [r/Fe] show mild decreasing trends, since the mass of the initial r-process elements in each of the clouds is close to or higher than the yields of the single main r-process event.

2. Based on the assumptions of (1) the progenitor of the SN II-Fe event does not produce the main r-process elements and (2) the yields of the SN II-Fe event possess the primary nature, we find that the observed lower boundaries of [r/Fe] can be explained. For the

clouds with the initial metallicities $[\text{Fe}/\text{H}] \lesssim -2.5$, the lower boundaries of $[\text{r}/\text{Fe}]$ show sharp increasing trends, since the initial Fe mass in each of the clouds is lower than the Fe yield of the single SN II-Fe event. On the other hand, for the clouds with the initial metallicities $[\text{Fe}/\text{H}] > -2.5$, the lower boundaries of $[\text{r}/\text{Fe}]$ show mild increasing trends, since the initial Fe mass in each of the clouds is close to or higher than the Fe yield of the single SN II-Fe event.

3. The observed upper and lower boundaries of $[\text{r}/\text{Fe}]$ present the extreme situations of the chemical enrichment in the early Galaxy. The calculated results mean that, for a cloud from which metal-poor stars formed, the formation of the upper limits of $[\text{r}/\text{Fe}]$ is mainly due to the pollution from a single main r-process event. For a cloud from which metal-poor stars formed, the formation of the lower limits of $[\text{r}/\text{Fe}]$ is mainly due to the pollution from a single SN II-Fe event.

Our results may provide useful clues for investigating the star formation history and the early Galactic chemical evolution. Obviously, more observational and theoretical studies of the main r-process event and the SN II-Fe event are desirable.

This work has been supported by the National Natural Science Foundation of China under Grants 11673007, 11273011, U1231119, 10973006, 11403007, 11547041, 11643007 and 11273026, the Natural Science Foundation of Hebei Province under Grant A2011205102, the Program for Excellent Innovative Talents in University of Hebei Province under Grant CPRC034, and the Innovation Fund Designated for Graduate Students of Hebei Province under Grant sj2016023.

REFERENCES

- Aoki, W., Beers, T. C., Honda, S., et al. 2010, *ApJL*, 723, L201
- Argast, D., Samland, M., Gerhard, O. E., & Thielemann, F. K. 2000, *A&A*, 356, 873
- Arlandini, C., Käppeler, F., Wisshak, K., et al. 1999, *ApJ*, 525, 886
- Barklem, P. S., Christlieb, N., Beers, T. C., et al. 2005, *A&A*, 439, 129
- Beniamini, P., Hotokezaka, K., & Piran, T. 2016a, *ApJL*, 829, L13
- Beniamini, P., Hotokezaka, K., & Piran, T. 2016b, *ApJ*, 832, 149
- Burbidge, E. M., Burbidge, G. R., Fowler, W. A., et al. 1957, *RvMP*, 29, 547
- Burris, D. L., Pilachowski, C. A., Armandroff, T. E., et al. 2000, *ApJ*, 544, 302
- Busso, M., Gallino, R., & Wasserburg, G. J. 1999, *ARA&A*, 37, 239
- Christlieb, N., Beers, T. C., Barklem, P. S., et al. 2004, *A&A*, 428, 1027
- Cohen, J. G., Christlieb, N., Thompson, I., et al. 2013, *ApJ*, 778, 56
- Cowan, J. J., Thielemann, F. K., & Truran, J. W. 1991, *PhR*, 208, 267
- Cowan, J. J., Sneden, C., Burles, S., et al. 2002, *ApJ*, 572, 861
- Cescutti, G., François, P., Matteucci, F., et al. 2006, *A&A*, 448, 557
- Cescutti, G. 2008, *A&A*, 481, 691
- Eichler, D., Livio, M., Piran, T., & Schramm, D. N. 1989, *Natur*, 340, 126
- Fields, B. D., Truran, J. W., & Cowan, J. J. 2002, *ApJ*, 575, 845
- François, P., Depagne, E., Hill, V., et al. 2007, *A&A*, 476, 935
- Gilroy, K. K., Sneden, C., Pilachowski, C. A., & Cowan, J. J. 1988, *ApJ*, 327, 298
- Goriely, S., & Janka H. T. 2016, *MNRAS*, 459, 4174G
- Hansen, C. J., Montes, F., & Arcones, A. 2014, *ApJ*, 797, 123H
- Hansen, C. J., Primas, F., Hartman, H., et al. 2012, *A&A*, 545, A31
- Hansen, T., Hansen, C.J., Christlieb, N., et al. 2015, *ApJ*, 807, 173
- Hayek, W., Wiesendahl, U., Christlieb, N., et al. 2009, *A&A*, 504, 511
- Heger, A., & Woosley, S. E. 2010, *ApJ*, 724, 341

- Hill, V., Plez, B., Cayrel, R., et al. 2002, *A&A*, 387, 560
- Hollek, J. K., Frebel, A., Roederer, I. U., et al. 2011, *ApJ*, 742, 54
- Honda, S., Aoki, W., Kajino, T., et al. 2004, *ApJ*, 607, 474
- Honda, S., Aoki, W., Ishimaru, Y., et al. 2006, *ApJ*, 643, 1180
- Honda, S., Aoki, W., Ishimaru, Y., & Wanajo, S. 2007, *ApJ*, 666, 1189
- Hotokezaka, K., Piran, T., & Paul, M. 2015, *NatPh*, 11, 1042
- Ishimaru, Y., Wanajo, S., & Prantzos, N. 2015, *ApJL*, 804, L35
- Ivans, I., Simmerer, J., Sneden, C., et al. 2006, *ApJ*, 645, 613
- Johnson, J. 2002, *ApJS*, 139, 219
- Jacobson, H., Keller, S., Frebel, A., et al. 2015, *ApJ*, 807, 171
- Ji, A. P., Frebel, A., Chiti, A., & Simon, J. D. 2016, *Natur*, 531, 610
- Käppeler, F., Beer, H., & Wisshak, K. 1989, *RPPh*, 52, 945
- Kobayashi, C., Umeda, H., Nomoto, K., et al. 2006, *ApJ*, 653, 1145
- Komiya, Y., Yamada, S., Suda, T., & Fujimoto, M. Y. 2014, *ApJ*, 783, 132
- Komiya, Y., & Shigeyama, T. 2016, *ApJ*, 830, 76
- Lamb, S., Howard, W. M., Truran, J. W., et al. 1977, *ApJ*, 217, 213
- Lai, D. K., Bolte, M., Johnson, J. A., et al. 2008, *ApJ*, 681, 1524
- Lattimer, J. M., & Schramm, D. N. 1974, *ApJ*, 192, L145
- Li, H. N., Zhao, G., Christlieb, N., et al. 2015a, *ApJ*, 798, 110
- Li, H. N., Aoki, W., Honda, S., et al. 2015b, *RAA*, 15, 1264L
- Li, H. J., Cui, W. Y., & Zhang, B. 2013a, *ApJ*, 775, 12
- Li, H. J., Shen, X. J., Liang, S., et al. 2013b, *PASP*, 125, 143
- Li, H. J., Ma, W. J., Cui, W. Y., et al. 2014, *PASP*, 126, 544
- Machida, M. N., Tomisaka, K., Nakamura, F., & Fujimoto, M. Y. 2005, *ApJ*, 622, 39
- Mashonkina, L., Christlieb, N., Barklem, P. S., et al. 2010, *A&A*, 516, 46
- Mashonkina, L., Christlieb, N. & Eriksson, K. 2014, *A&A*, 569, A43
- Mathews, G. J., Bazan, G., & Cowan, J. J. 1992, *ApJ*, 391, 719
- McWilliam, A., Preston, G. W., Sneden, C., et al. 1995, *AJ*, 109, 2757
- McWilliam, A. 1998, *AJ*, 115, 1640
- Mishenina, T. V., Pignatari, M., Korotin, S. A., et al. 2013, *A&A*, 552, A128
- Montes, F., Beers, T. C., Cowan, J., et al. 2007, *ApJ*, 671, 1685
- Nomoto, K., Kobayashi C. & Tominaga, N. 2013, *ARA&A*, 51, 457
- Qian, Y. Z., Vogel, P., & Wasserburg, G. J. 1998, *ApJ*, 494, 285
- Qian, Y. Z., & Wasserburg, G. J. 2001, *ApJ*, 559, 925
- Qian, Y. Z., & Wasserburg, G. J. 2007, *PhR*, 442, 237
- Raiteri, C. M., Busso, M., Gallino, R., et al. 1991, *ApJ*, 367, 228
- Raiteri, C. M., Gallino, R., Busso, M., et al. 1993, *ApJ*, 419, 207
- Ramirez-Ruiz, E., Trenti, M., MacLeod, M., et al. 2015, *ApJL*, 802, L22
- Roederer, I. U., Sneden, C., Thompson, I. B., et al. 2010, *ApJ*, 711, 573
- Roederer, I. U., Preston, G. W., Thompson, I. B. 2014, *AJ*, 147, 136
- Rosswog, S., Korobkin, O., Arcones, A., et al. 2014, *MNRAS*, 439, 744

- Ryan, S. G., Norris, J. E., & Beers, T. C. 1996, *ApJ*, 471, 254
- Siqueira-Mello, C., Barbuy, B., Spite, M., & Spite, F. 2012, *A&A*, 548, A42
- Siqueira-Mello, C., Chiappini, C., Barbuy, B., et al. 2016, *A&A*, 593, A79
- Snedden, C., Cowan, J. J., Burris, D. L., & Truran, J. W. 1998, *ApJ*, 496, 235
- Snedden, C., Cowan, J. J., Lawler, J. E., et al. 2003, *ApJ*, 591, 936
- Snedden, C., Cowan, J. J., & Gallino, R. 2008, *ARA&A*, 46, 241
- Snedden, C., Preston, G. W., McWilliam, A., & Searle, L. 1994, *ApJL*, 431, L27
- Travaglio, C., Galli, D., Gallino, R., et al. 1999, *ApJ*, 521, 691
- Travaglio, C., Galli, D., & Burkert, A. 2001, *ApJ*, 547, 217
- Travaglio, C., Gallino, R., Arnone, E., et al. 2004, *ApJ*, 601, 864
- Truran, J. W. 1981, *A&A*, 97, 391
- Tsujimoto, T., Shigeyama, T., & Yoshii, Y. 1999, *ApJ*, 519, L63
- Tsujimoto, T., & Shigeyama, T. 2014a, *ApJL*, 795, L18
- Tsujimoto, T., & Shigeyama, T. 2014b, *A&A*, 565, L5
- Wanajo, S., Tamamura, M., Itoh, N., et al. 2003, *ApJ*, 593, 968
- Wasserburg, G. J., Busso, M., & Gallino, R. 1996, *ApJL*, 466, L109
- Westin, J., Snedden, C., Gustafsson, B., et al. 2000, *ApJ*, 530, 783
- Woodsley, S. E., & Weaver, T. A. 1995, *ApJS*, 101, 181
- Yong, D., Norris, J. E., Bessell, M. S., et al. 2013, *ApJ*, 762, 26

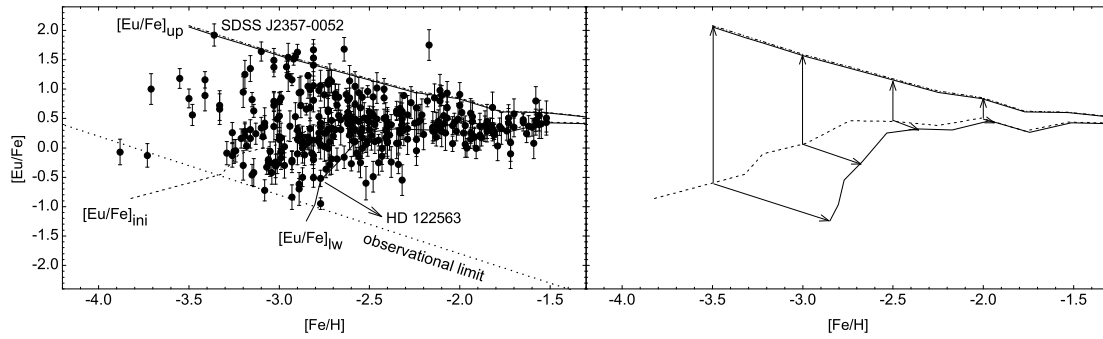


Fig. 1.— $[Eu/Fe]$ ratios as a function of $[Fe/H]$ for the metal-poor stars. In the left panel, the filled circles represent the observed abundance ratios. The dashed line refers to the initial $[Eu/Fe]$ ratios of the clouds. The upper solid line and dotted-dashed line are the calculated upper boundaries of $[Eu/Fe]$ for the clouds swept up by the SNe II with the progenitor mass $M \approx 8 - 10 M_{\odot}$ and NSMs, respectively. The lower solid line is the calculated lower boundary of $[Eu/Fe]$. The dotted line with -1 slope represents the sensitivity limit for observing Eu. In the right panel, the lines have the same meaning as in the left panel. Each up arrow represents the jump of $[Eu/Fe]$ in a cloud swept up by a single main r-process event. Each inclined arrow represents the jumps of $[Eu/Fe]$ and $[Fe/H]$ in a cloud swept up by a single SN II-Fe event.

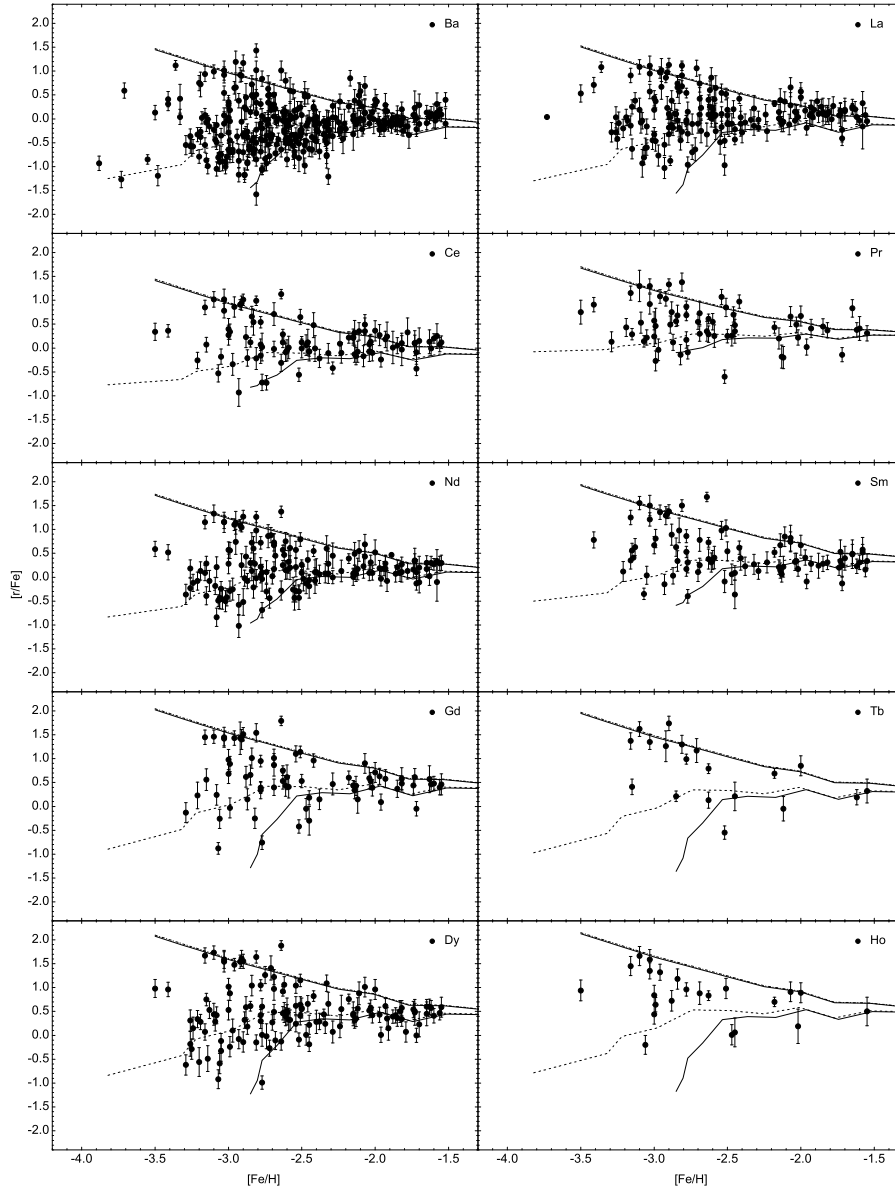


Fig. 2.— The same as in the left panel of Figure 1, but for the $[r/\text{Fe}]$ ratios (r : Ba, La, Ce, Pr, Nd, Sm, Gd, Tb, Dy and Ho).

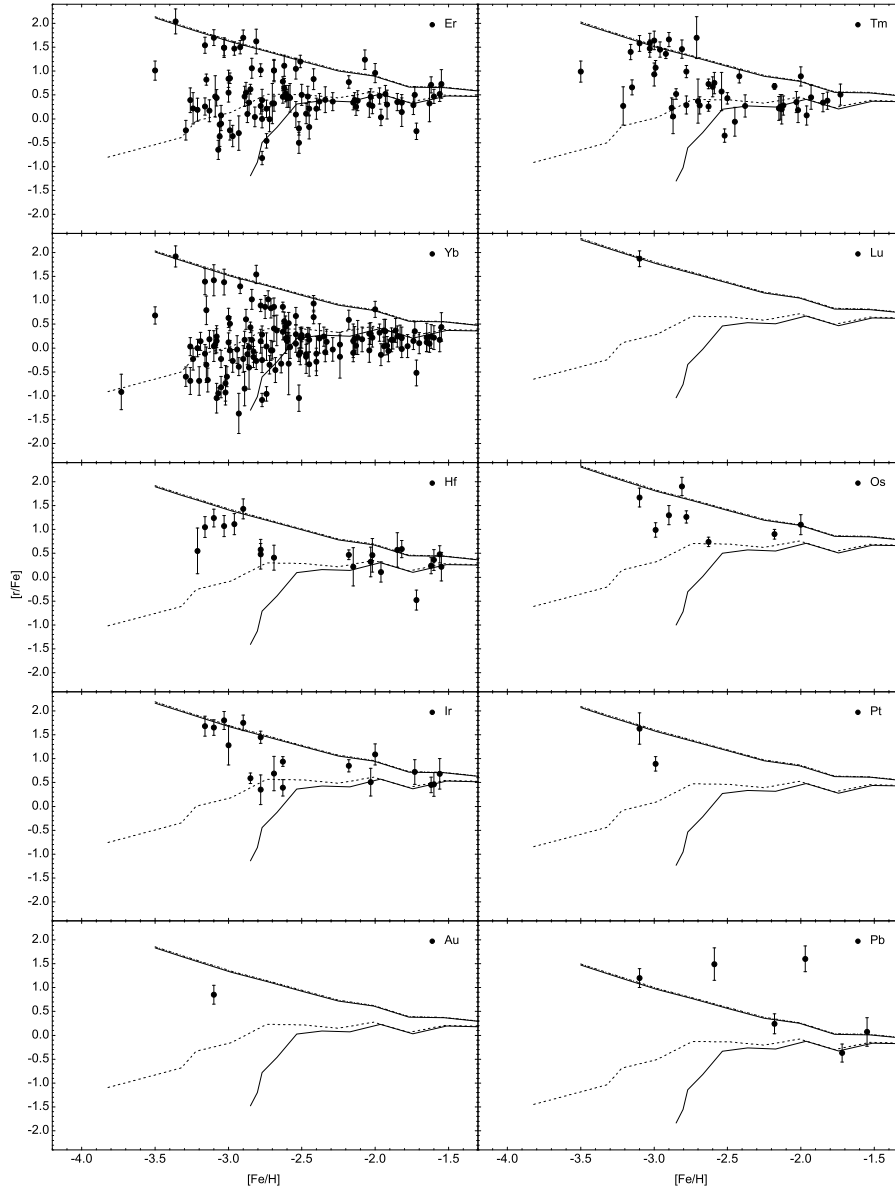


Fig. 3.— The same as in the left panel of Figure 1, but for the $[r/Fe]$ ratios (r : Er, Tm, Yb, Lu, Hf, Os, Ir, Pt, Au and Pb).